Classification: BIOLOGICAL SCIENCES

Title: Autism sensory dysfunction in an evolutionarily conserved system

Authors

Greta Vilidaite[a]*†, Anthony M. Norcia[b]*†, Ryan J. H. West[c], Christopher J. H. Elliott[c], Francesca Pei[d], Alex R. Wade[a,c], & Daniel H. Baker[a]

Author affiliations

[a] Department of Psychology, University of York, York, YO10 5DD, UK.

[b] Department of Psychology, Stanford University, CA 94305, USA.

[c] Department of Biology, University of York, York, YO10 5DD, UK.

[d] Department of Psychiatry, Stanford University, CA 94305, USA.

† Authors contributed equally

Corresponding authors

* Correspondence and requests for materials should be addressed to gv529@york.ac.uk or amnorcia@stanford.edu

Key words

Autism, animal model, sustained, *Drosophila*, sensory processing, visual system

Abstract

Individuals with Autism Spectrum Disorder (ASD) report a host of sensory symptoms, which suggests a fundamental, genetic (Miles, 2011) neural signaling deficit in autistic brains (Rubenstein & Merzenich, 2003). However, neither animal models nor previous theories explaining sensory symptoms have been able to predict neurophysiological data in autistic humans. Here we show a strikingly similar trajectory of visual development in a genetic *Drosophila Nhe3* model of autism and in autistic human participants. We report a dissociation between first- and second-order electrophysiological visual responses to steady-state stimulation in adults with ASD as well as a large sample of neurotypical individuals with high numbers of autistic traits. We also report a strikingly similar impairment in the adult fruit fly model of ASD. We explain this as a selective signaling abnormality in the transient response mechanisms in the visual system. In contrast to adults, autistic children show decreases in both first- and second-order responses, which are closely matched by the fruit fly model, suggesting a compensatory change in processing occurs over the course of development. Our results provide the first animal model of autism comprising a developmental sensory pathway phenotype.

Significance statement

Autism Spectrum Disorder exhibits strong and widespread sensory symptoms that have not yet been explained by previous research. Here we have developed a novel *Drosophila* model of sensory deficits in autism that is highly predictive of electrophysiological visual data in both autistic adults and children. Both the animal model, and human data from three samples (total N=154), point towards a deficit of a fundamental signaling mechanism in early parts of the sensory system. This deficit shows signs of change during development indicating a possible partial rescue of function at later stages of life. Our findings can explain previous inconsistencies in research into visual perception in autism. The *Drosophila* model can be used in future biomarker and treatment development.

Introduction

Autistic individuals report a host of sensory symptoms including unusual sensory interests, overstimulation and hyper- and hyposensitivity to intense stimuli such as bright lights or loud noises (*1*, *2*). Several theories have been proposed to account for sensory abnormalities in autism – one of the most common proposing an imbalance in excitation/inhibition (E/I) (*3*). The E/I imbalance theory of autism has gained mixed but largely supportive evidence from neurochemical, neurobiological and genetic investigations (*4*, *5*), implicating GABA-ergic mechanism deficits (*6*). Alternatively, a vision-specific theory has linked visual processing abnormalities in ASD to a selective deficit in the magnocellular pathway (*7*, *8*). Such signaling-level impairments indicate a genetic cause of ASD sensory symptoms (*9*). However, neural measurements that can convincingly delineate these competing explanations are yet to be reported.

One attempt in mice to model a related developmental condition, Rett syndrome, found similar cross-species decreases in visual neural responses and poor visual acuity (*10*). However, Rett syndrome lacks the pervasive sensory symptoms characteristic of autism, thus it is difficult to link cellular and genetic abnormalities to ASD sensory deficits (*11*). As an alternative to rodents, *Drosophila* have provided successful models of human neurological disorders such as Parkinson's (*12*) and Alzheimer's (*13*). Fruit flies share 75% of human disease causing genes (*14*) and have a visual system exhibiting similar nonlinear neural properties, including a color- and luminance-selective module as well as a motion-selective module (*15*). The neural dynamics of these modules closely resemble those of the transient and sustained neural populations in humans (*16*–*18*). This provides an excellent framework for modeling low-level changes in sensory neuronal signaling (*18*) which may lie behind sensory abnormalities in autism.

In this study we aimed to develop an animal model of sensory abnormalities in human ASD and to investigate the mechanism underlying these impairments. We measured visual neural responses both in autistic humans and in *Drosophila* with a genetic mutation linked to autism. In humans, loss-of-function mutations in the gene *SLC9A9* have been linked to ASD (*19*). Here we used a *Drosophila* orthologue of *SLC9A9* – *Nhe3*. A homozygous P-element insertion loss-of-function mutants ($Nhe3^{KG08307}$) and *Nhe3* hemizygotes ($Nhe3^{KG08307}$/Df(2L)BSC187) were used to inhibit *Nhe3* function in fly. To assess the functionality of sustained and transient pathways in these species, we measured two steady-state electrophysiological responses: first harmonic (stimulation) and second harmonic frequencies, in both humans and fruit flies. The use of two *Nhe3* mutations in different genetic backgrounds

ruled out the possibility of other mutations influencing the flies' visual responses. The dynamics of the sustained pathway manifest in the electrophysiological stimulation frequency (first harmonic) response whereas the dynamics of the transient pathway can be observed in the second harmonic response (*17*, *20*). Furthermore, to investigate the progression of ASD sensory abnormalities over the course of development, we also measured visual responses at two stages of fruit fly maturation and acquired similar responses from autistic children. Finally, as the ASD phenotype is complex and non-binary, we validated our sensory model with a large sample of neurotypical participants with high and low numbers of autistic traits.

Results

Increased sustained/transient response ratio in *Nhe3* fruit flies. Using a steady-state visual evoked potential (ssVEP) paradigm (*12*) (see *Fig. 1*) we measured fruit fly visual responses to flickering stimuli via an electrode on the fly's eye. Wild type, eye-color matched flies (a cross between isogenic and Canton-S) were used as controls (+). Flies from each genotype (n=12) were tested at three days (when the flies are young) and at 14 days post eclosion (older). First harmonic (12Hz) and second harmonic (24Hz) response amplitudes were derived by fast Fourier transform (see *Methods*). Although the first harmonic responses of mutant and wild-type flies were the same, the second harmonic response was significantly reduced in the *Nhe3* mutants (*Fig. 2a, 2b*).

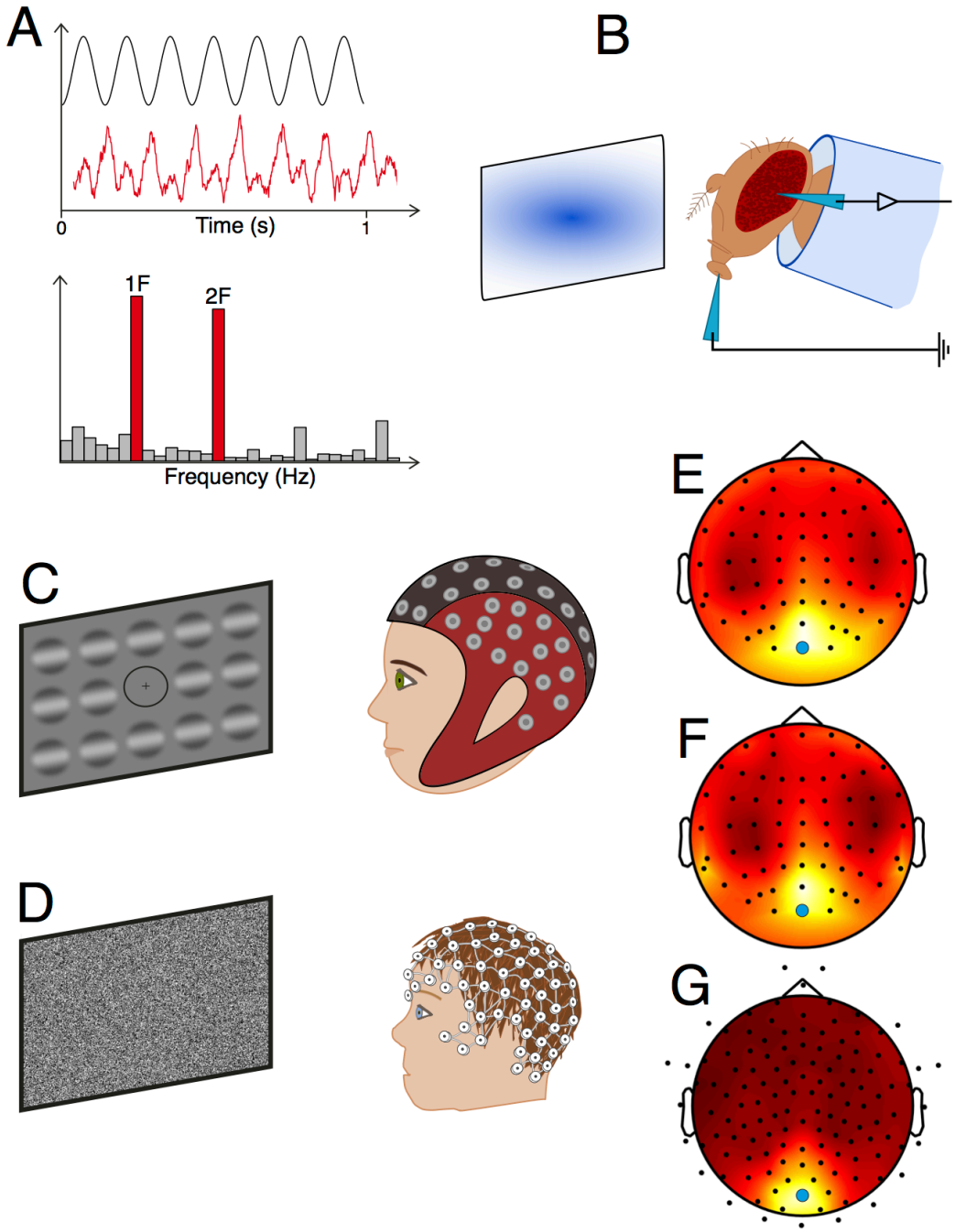

Figure 1. Human and *Drosophila* steady-state electrophysiology methods.

To quantify this functional dissociation between the two response components we calculated a normalized ratio between first (1F) and second (2F) harmonics ($\frac{1F-2F}{1F+2F}$) and averaged over the highest contrast conditions (where the response rises above the noise floor, see *Methods*). This allowed us to measure the differences between sustained and transient responses whilst normalizing for overall responsiveness of the visual pathway. The ratio was

significantly higher in both mutant strains than in the controls (ANOVA, $F_{2,33}$ = 20.53, P < 0.0001, both paired contrasts P < 0.001; *Fig. 2c*). These data suggest an impairment in the post-receptoral neural pathways (structures downstream of the photoreceptors) of the older mutant flies.

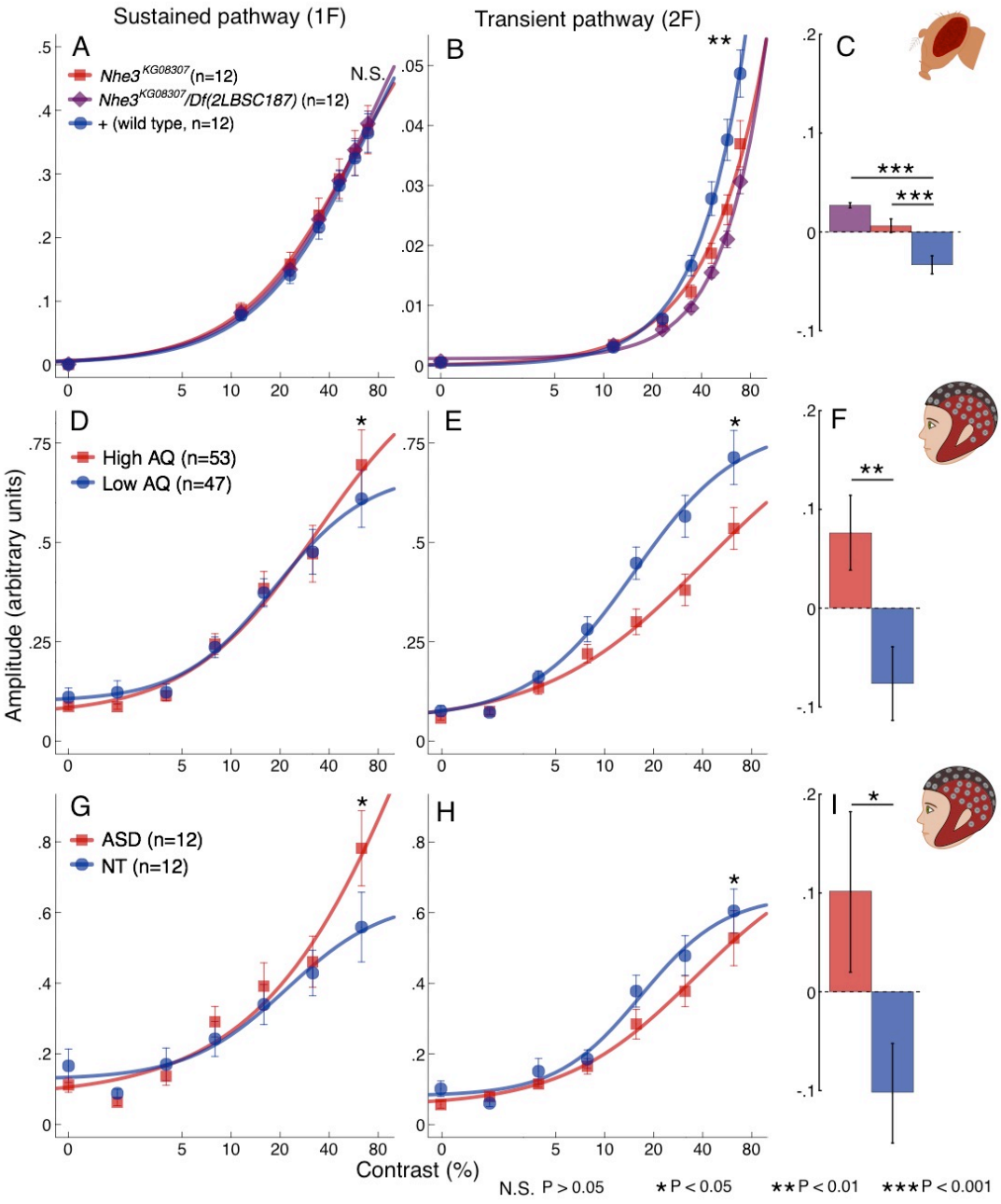

Figure 2. Older ASD-mimic flies and autistic humans have visual deficits in the transient pathway.

Interestingly, unlike the older flies, the young 3 day old flies showed a reduced response at both frequencies (see *Fig. 3a,b*) relative to controls. Importantly,

there was no effect of genotype on the ratio between harmonics ($F_{2,33}$ = 1.38, P = 0.27; *Fig. 3c*). These results suggest a deficit in the sustained visual module of young mutant flies, which most likely causes a cascading impairment in the transient module. These differences between visual responses at two stages of life suggest a change in visual processing over the course of development.

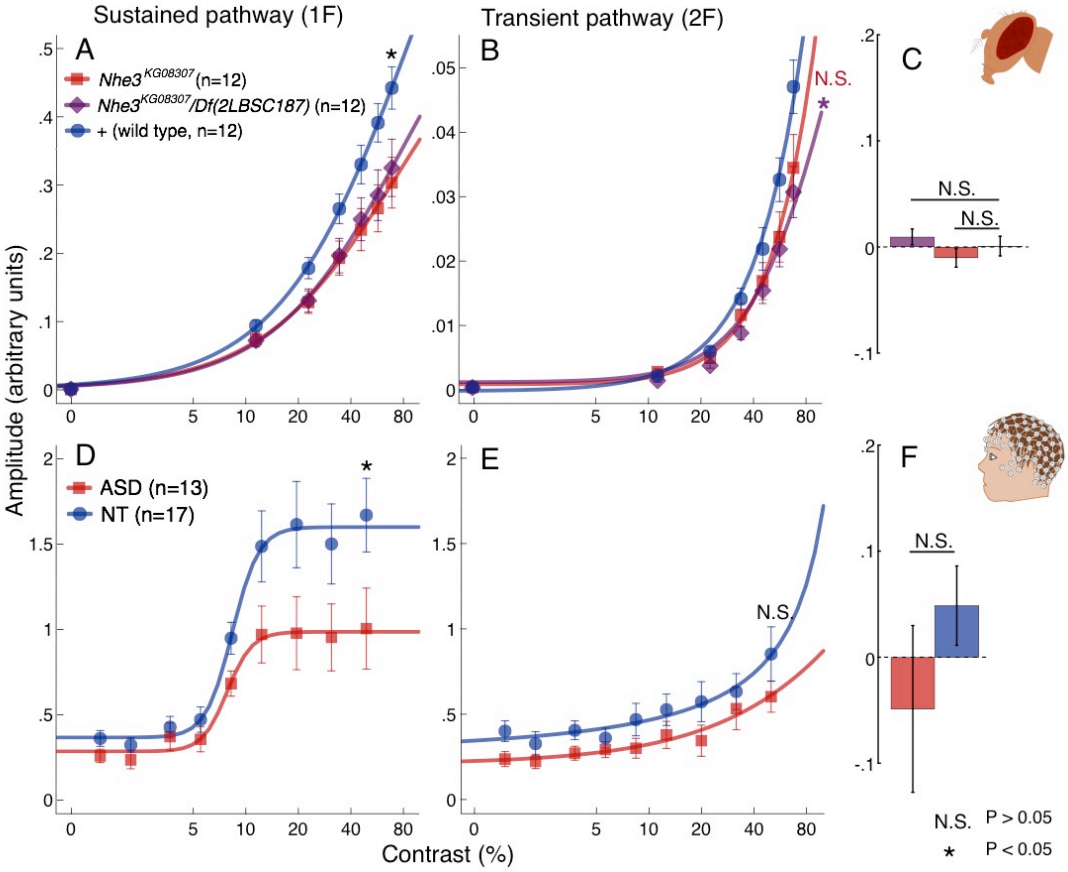

Figure 3. Young ASD-mimic flies and autistic children have visual deficits in the sustained pathway.

High autistic trait population show similar ssVEPs to *Nhe3* flies. To assess the relevance of the *Nhe3* model to the human ASD phenotype we used a comparable and equally sensitive steady-state EEG paradigm in human participants. One hundred neurotypical participants with putative autistic traits measured using the Autism Spectrum Quotient (AQ) questionnaire (*21*) were tested with the ssVEP paradigm. Visual responses were recorded from an occipital electrode (Oz, located at the back of the head over the visual cortex) to grating stimuli flickered at 7Hz. Seven contrast conditions (each repeated eight times) were presented in a randomized order. First and second harmonic ssVEP responses were again derived via Fourier analysis. The evoked response data were averaged separately over

participants split by their median AQ score: high (n = 53, AQ mean = 11.53, SD = 3.68) and low (n = 47, AQ mean = 5.32, SD = 1.81) AQ (high AQ implying many autistic traits). The first harmonic response was similar in both groups whereas the second harmonic was notably reduced in the high AQ group (*Fig. 2d, 2e*). A two-way ANOVA showed the interaction between group and frequency to be significant ($F_{1,98}$ = 6.17, P = 0.015). The high AQ group also had a significantly higher frequency ratio than the low AQ group (t_{98} = 2.86, P < 0.01, *Fig. 2f*). Moreover, a regression analysis showed that AQ scores correlated with the frequency ratio, with high AQ scores being predictive of higher ratios (R = 0.26 $F_{1,98}$ = 6.87, P = 0.01; see *Fig. 4*). This result shows a relationship between the amplitude of the second harmonic response and the severity of the subclinical ASD phenotype, however, this effect cannot be directly generalized to clinical autism as the AQ is not diagnostic of full-blown ASD.

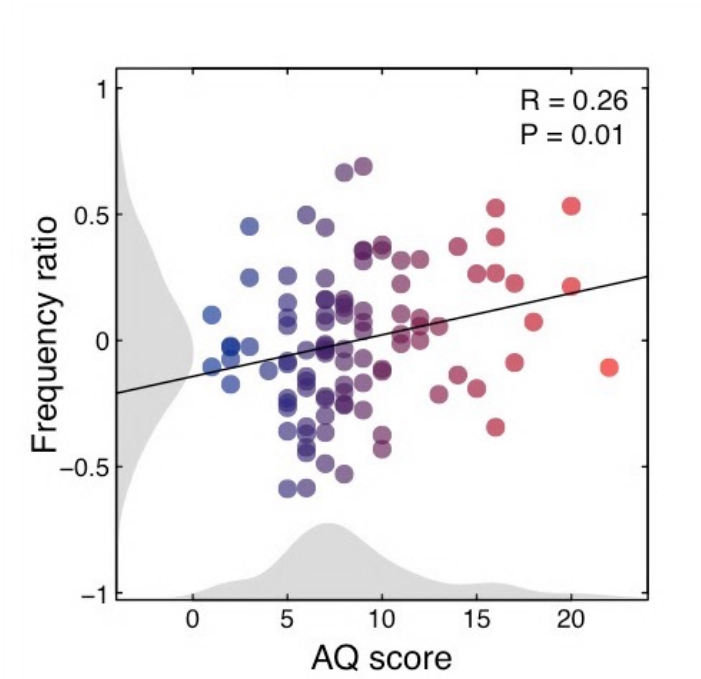

Figure 4. Positive relationship between the number of autistic traits and first/second harmonic ratio.

Autistic individuals show the same pattern of responses as *Nhe3* flies. We assess this difference between harmonics in clinical ASD by testing 12 typical-IQ autistic adults (diagnosis confirmed with the Autism Diagnostic Observation Schedule, Second Edition (ADOS-2), Lord et al., 2000) and 12 age- and gender-matched controls using the same human ssVEP paradigm. The pattern of data again mimicked that of the previous adult datasets: there was a significant interaction between group and frequency ($F_{1,22}$ = 5.85, P =

0.02; *Fig. 2g, 2h*). The ratio between harmonics was again significantly larger in the ASD group than in the control group (t_{22} = 2.13, P = 0.04; *Fig. 2i*).

Young *Nhe3* fly responses predict autistic children's responses. Considering the striking similarity between the adult human datasets and the adult fruit fly model, it is reasonable to ask if similarities also exist between younger humans and young Drosophila ASD models. Specifically, our fly model predicts that the visual system of autistic children should show reduced responses in both the first and second harmonics. To examine this, we recorded from 13 autistic children (5 – 13 years old) and 17 neurotypical age- and gender-ratio-matched controls using an ssVEP contrast-sweep paradigm. Artifact rejection was employed to control for movement and blinking in both groups. The stimulus in each sweep trial increased continuously in contrast from 0% to 50% in logarithmic steps. Data were binned into 9 contrast levels before being Fourier transformed to compute response amplitudes.

As predicted by the fly data, the ASD group showed impaired processing in the sustained response (t_{28} = 2.07, P = 0.04; *Fig. 3d, 3e*). A two-way ANOVA also revealed a significant group effect over both frequencies ($F_{1,28}$ = 4.23, P = 0.049). Unlike adults, children exhibited no difference in frequency ratios between the groups (t = 1.41, P = 0.17; *Fig. 3f*). Children showed impaired processing in the sustained pathway as predicted by the fruit fly model. However, the smaller effect of amplitude reduction observed in the fruit fly second harmonic responses was present, but not statistically reliable in the children (t_{28} = 1.26, P = 0.219). This may be due to the more variable nature of human EEG data.

Discussion

We found a selective deficit in second order responses in autistic adults, individuals with high levels of autistic traits and *Nhe3* fruit flies suggesting that this impairment is specific to the autistic phenotype. Autistic children and young *Nhe3* flies showed a more global deficit in visual processing at early stages of life. The *Nhe3* fruit fly model of autism was predictive of these ASD visual response deficits both in children and in adults, suggesting a fundamental and pervasive change in visual impairment during development. High AQ individuals showed consistent visual responses compared to participants with diagnosed ASD suggesting common visual response properties between samples. This was unsurprising as previous research has found that AQ scores in the general population are highly correlated (R = 0.77) with sensory processing difficulties, as measured by the Glasgow

Sensory Questionnaire (*23*), indicating that high AQ individuals exhibit milder forms of sensory difficulties.

The intact first harmonic response in adult flies and humans indicates normal functioning of mechanisms which give rise to the sustained response. Conversely, the reduced second harmonic response suggests a deficit in the transient dynamics of the visual system. In fly, the first harmonic has been associated with sustained photoreceptor polarization and the second harmonic with second-order lamina cells (*17*). In human, an association has been made between simple cell and sustained responses to pattern onset and complex cells and transient responses at both stimulus onset and offset (*24*). Although simple cells exhibit some transient response properties as well (*24*, *25*), the intact first harmonic suggests that the impairment is specific to human complex cells that only generate even-order response components. This early, cell-type-specific deficit may explain previous findings of atypical neural dynamics of spatial frequency processing in ASD in the face of normal sensitivity thresholds (*26*, *27*).

The differential impairment of sustained and transient modules observed in our *Nhe3* model mimics the pathway abnormality in autistic adults. *Nhe3* affects the exchange of sodium and hydrogen ions in cell membranes directly affecting neural signaling (*19*, *28*). Differential expression of *Nhe3* and other genes in ASD, which has been observed in other parts of the brain (*19*, *29*) may extend to differential expression in color and motion modules in the *Drosophila* visual system. As *Nhe3* (*SLC9A9* in humans) is only a single gene in a multifaceted genetic etiology of autism, it is likely that the expression of several genes in human autism affects simple and complex cell dynamics, producing similar effects at the neural population level. Furthermore, such abnormality in gene expression in other parts of autistic brains, as well as environmental influences and gene-environment interactions, may give rise to a wide range of cognitive and social impairments in childhood and adulthood.

Our data indicate little or no over-responsivity in the visual responses predicted by the E/I theory, consistent with some previous studies (*30*, *31*). However, it is possible that E/I imbalance in autism, stemming from GABA-ergic mechanism deficits, affects different neuron types or processing pathways in distinct ways and to different extents. Regardless, cell-type level processing abnormalities may explain previous inconsistencies in sensory deficits in ASD in which pathways were not differentiated (*32*). Furthermore, the current results can provide an amended explanation to the magnocellular (M pathway) dysfunction hypothesis. As it is difficult to isolate the M pathway

by changing stimulus properties (*20*), the paradigms previously used to investigate magnocellular dysfunction in ASD may have been selectively activating complex cells rather than the M pathway in particular (*33*, *34*).

Developmentally, the observed change in the nature of the abnormality in both species with increasing age is in accordance with previous findings showing reduction or complete rescue of neuroanatomical abnormalities present in early ASD childhood over the course of maturation (*35*). Previous longitudinal research has also shown that symptom severity in individuals diagnosed with ASD in childhood decreases over time (*36*, *37*). McGovern & Sigman (*37*) found that 48 adolescents, who were diagnosed with ASD as children, showed marked improvement in social interaction, repetitive/stereotyped behaviors and other symptoms, with two no longer meeting criteria for ASD under ADI-R criteria, and four under ADOS criteria. This might be explained by a change in neural processing during development, which would likely affect both behavioral and sensory outcomes.

One possible mechanism that would explain the present results is that the neural signaling abnormalities (such as ion balance in the case of *Nhe3*), change over time. In flies, reduced *Nhe3* expression may reduce the rate at which sodium ions and protons are exchanged across the cell membrane. At least in Mosquito, this exchanger is found in the gut, and Malpighian tubules (the fly equivalent of the kidney) (*38*). Failure to properly regulate ionic balance in young adult flies might affect the sodium concentration, or proton levels in the body and brain, and affect the speed an intensity of action potentials. Later in life, the normal balance may be restored. A similar reduction in efficacy of *SLC9A9,* linked to ASD, may also be present and explain the homology. In this respect, we note that another transporter, the potassium/chloride exchanger, has been linked to epilepsy in young people: with age the kcc/KCC2 eventually achieves a normal ionic balance and proper inhibitory GABA signaling (*39*).

The *Nhe3* model may serve for further research into the development of ASD in young brains as well as early biomarkers and treatments. Consistency between the fly and human datasets at both ages indicates a breakdown of a fundamental sensory mechanism comprising two components that have been conserved over 500 million years of evolution. The conservation of the phenotype and mechanisms from fly to human opens up the option to utilize the unrivaled genetic tractability of the fly to dissect the molecular mechanisms underpinning the disorder.

Methods

Drosophila stocks

Two *Drosophila melanogaster* genotypes were used as ASD models. The *Nhe3* loss-of-function P-element insertion (*Nhe3*^{KG08307} homozygotes) mutation was homozygous *P{SUPor-P}Nhe3*^{KG08307} (Bloomington Drosophila Stock Center (BDSC) 14715). The deficiency was Df(2L)BSC187 (BDSC 9672). To avoid second site mutations in the P-element stock, we used the hemizygote *Nhe3*^{KG08307} */Df(2L)BSC187* as a second experimental genotype.

For our control cross we mated the lab stock of *Canton-S (CS*) flies with those with isogenic chromosomes 2C and 3J (*40*). All tested flies had dark red eyes. All genotypes were raised in glass bottles on yeast-cornmeal-agar-sucrose medium (10g agar, 39g cornmeal, 37g yeast, 93.75g sucrose per litre). They were kept at 25°C on a 12 hour light-dark cycle. Male flies were collected on CO_2 the day after eclosion and placed on Carpenter (1950) (*41*) medium in the same environmental conditions for either 3 days or 14 days. Flies were tested approximately between the 4th and 9th hour of the daylight cycle.

Drosophila electroretinography

Steady-state visual evoked potentials (SSVEPs) were obtained from the fruit flies (*12*, *17*). Flies were recorded in pairs in a dark room. They were placed in small pipette tips and secured in place with nail varnish. One glass saline-filled electrode was placed inside the proboscis of the fly and another on the surface of the eye. A blue (467nm wavelength) LED light (Prizmatix FC5-LED) with a Gaussian spectral profile (FWHM 34nm) was placed in front of the flies together with a diffuser screen and used for temporal contrast stimulation. Flies were dark adapted for at least two minutes and then tested for signal quality with six light flashes. Steady-state stimulation lasted 12 min and comprised seven contrast levels (0 – 69% in linear steps) each with five repetitions. The frequency of the light flicker was 12Hz. Each trial (contrast level repetition) was 11 s. The order of the contrast conditions was randomized. The stimulation and the recording from the fly was controlled by in-house MATLAB scripts (scripts can be found in https://github.com/wadelab/flyCode).

Adult EEG

One-hundred neurotypical adult participants (32 males, mean age 21.87, range 18 – 49, no reported diagnosis of ASD, reportedly normal or corrected

to normal vision) took part in the autism spectrum quotient (AQ) measurement study. The AQ is an instrument used for quantifying autistic traits in the neurotypical population and has been shown to have high face validity and reliability in these populations (*21*). The AQ consists of 50 Likert scale items and the scores in this study were calculated according to Baron-Cohen et al. (*21*). Each participant completed the AQ questionnaire on a computer in the laboratory.

For the autistic adult ssVEP study, 12 typical-IQ autistic participants and 12 gender- and age- matched controls (11 males, mean age 23.53, range 18 – 39, reportedly normal or corrected to normal vision) took part. ASD diagnosis was confirmed with the Autism Diagnostic Observation Schedule, second edition (ADOS-2). Although IQ was not explicitly measured in this study, all adults had normal speech and a high level of independence (the majority were university students). The absence of ASD diagnosis in the neurotypical participants was also confirmed with ADOS-2 (none of the control participants met criteria for ASD). All participants in the study gave informed consent and were debriefed on the purpose of the study after the experiment. The experiments were approved by the Department of Psychology Ethics Committee at the University of York.

Steady-state VEPs were recorded using an ANT Neuro system with a 64-channel Waveguard cap. EEG data were acquired at 1kHz and were recorded using ASALab, with stimuli presented using MATLAB. The timing of the recording and the stimulation was synchronized using 8-bit low-latency digital triggers. All sessions were performed in a darkened room, testing lasted 45-60min with approximately 20min set up time.

Stimuli were presented on a ViewPixx display (VPixx Technologies Inc., Quebec, Canada) with a mean luminance of 51cd/m^2 and a refresh rate of 120Hz. Stimuli were 0.5 cycle/deg sine-wave gratings enveloped by a raised cosine envelope. Gratings subtended 3 degrees of visual angle and were tiled in a 17x9 grid. The participants fixated on a circle in the middle of the screen and performed a fixation task (two-interval-forced-choice contrast discrimination) to maintain attention. All participants were able to perform the task at above chance levels. There were seven contrast conditions for the flickering gratings (0%, and 2 - 64% in logarithmic steps, where $C_{\%} = 100(L_{max}-L_{min})/(L_{max}+L_{min})$, L is luminance) and eight repetitions. Stimuli flickered on/off sinusoidally at 7Hz. Trials were presented in random order in four testing blocks with short breaks in between. Each trial was 11 seconds long and contained gratings of a random spatial orientation to avoid orientation adaptation effects. These trials were intermixed with orthogonal masking trials that are not presented as part of this study. Data were taken from the occipital electrode Oz.

Child EEG

Thirteen children with a diagnosis of ASD and 20 neurotypical controls matched on gender ratio (10 and 12 males respectively) and average age (mean age 9.31 and 8.94 respectively, range 5 – 13) completed the study. Three of the neurotypical children were tested but excluded due to having autistic siblings (17 participants were included). All children were in mainstream local schools (if they were old enough) and did not have other (or any – in the case of the neurotypical group) reported history of serious medical, psychiatric, or neurological conditions.

Steady state EEG data were acquired with a 128-channel HydroCell Geodesic Sensor Net (Electrical Geodesics Inc.). Data were digitized at 432Hz and band-pass filtered from 0.3Hz to 50Hz and were recorded using NetStation 4.3 Software. Highly noisy data were excluded by removing repetitions with amplitudes that were four standard deviations away from the group mean (for each contrast level and harmonic individually). There were 10 repetitions in total, however, two autistic and one neurotypical child only completed 8 repetitions.

Increasing contrast sweep ssVEPs were used. Stimuli for this experiment were presented on an HP1320 CRT monitor with 800x600 pixel resolution, 72Hz refresh rate and mean luminance of 50cd/m^2. Stimuli were random binary noise patterns of two luminance levels that increased in contrast in 9 logarithmic steps (0% – 50%) of 1 second each. Each trial contained a prelude at the initial value of the sweep and a postlude at the final sweep value, lasting 12 seconds in total. Stimuli flickered at 5.12Hz. Data from the middle 9 seconds during the sweep were binned according to contrast steps. Methodological differences between the adult and child datasets were due to different conventions being used by the two laboratories in which data were collected.

Data analysis

A Fast Fourier transform (in MATLAB) was used to retrieve steady-state response amplitudes at the stimulation frequency (12Hz for fruit flies, 7Hz for adult participants and 5.12Hz for children) and at the second harmonic (24Hz, 14Hz and 10.24Hz respectively). Fourier transforms were applied to 10 s of each trial (first 1s discarded; total trial length was 11s) for the fruit fly and the adult participant datasets and to 1 second binned data for the children's dataset. Contrast response functions were obtained by coherently averaging the amplitudes over repetitions for each contrast level within a participant. Group/genotype scalar means over response amplitude (discarding phase angle) were then calculated for each contrast across participants/flies.

Two-way (harmonic x group) ANOVAs were performed on amplitudes at the highest contrast level to investigate the interactions and group effects in all human datasets where only two groups were compared. To identify at which harmonic the autistic children showed a decreased response, two independent samples t-tests were also conducted. One-way ANOVAs with simple planned contrasts were conducted to assess the genotype differences in fruit fly first and second harmonic responses separately as that aided the interpretability of the results between the three genotypes.

To investigate the dissociation between first and second harmonic responses a scaled ratio $\frac{1F-2F}{1F+2F}$ (where 1F is the first and 2F is the second harmonic) was calculated for each participant/fly and each contrast condition. To increase the power of statistical analyses and to decrease the type I error rate, the ratios were then averaged over the contrast conditions that had first harmonic amplitudes significantly above the baseline response (0% contrast condition). For fruit flies this was six conditions (11.5 – 69%), for adult participants this was four conditions (8 – 64%) and for children this was five conditions (8.5 – 50%). This procedure resulted in a single frequency-ratio index for each participant/fly. One-way ANOVAs with simple planned contrasts (comparing mutant genotypes with the control genotype) were conducted on the fly frequency ratios for each age separately. Independent t-tests were used to compare frequency ratios in all human datasets between groups. Additionally, a linear regression was conducted on the adult AQ measurement dataset to assess the predictive power of AQ scores on the ratios between frequencies. All statistical tests were two-tailed.

Acknowledgements

This research was supported by the Experimental Psychology Society Study Visit Grant awarded to G.V.

We would like to thank E. Cole for second-coding ADOS2 assessments; N. Gutmanis, S. Harris, R.E. Kitching, H.A. Melton, R. Norman, C.J.T. Scott, C. Simpson, A.K. Smith, A. Stockton and K. Wailes-Newson for contributing to EEG data collection. A.M.N. and F.P. were supported by a grant from the Simons Foundation Autism Research Initiative. We would also like to thank the Experimental Psychology Society for awarding G.V. the Grant for Study Visits for travel to Stanford University. Lastly, we would like to thank all our participants and their families for their contribution.

References

1. Jones RSP, Quigney C, Huws JC (2003) First-hand accounts of sensory perceptual experiences in autism: a qualitative analysis. *Journal of Intellectual & Developmental Disability* 28(2):112-121.

2. Ben-Sasson A et al. (2008) A Meta-Analysis of Sensory Modulation Symptoms in Individuals with Autism Spectrum Disorders. *Journal of Autism and Developmental Disorders* 39:1-11.

3. Rubenstein JLR, Merzenich MM (2003) Model of autism: increased ratio of excitation/inhibition in key neural systems. *Genes, Brain and Behavior* 2(5):255-267.

4. Nelson SB, Valakh V (2015) Excitatory/Inhibitory Balance and Circuit Homeostasis in Autism Spectrum Disorders. *Neuron* 87(4):684-698.

5. Hahn N et al. (2013) Monogenic heritable autism gene neuroligin impacts Drosophila social behaviour. *Behavioural Brain Research* 252:450-457.

6. Gao R, Penzes P (2015) Common Mechanisms of Excitatory and Inhibitory Imbalance in Schizophrenia and Autism Spectrum Disorders. *Current Molecular Medicine* 15(2):146-167.

7. Plaisted K, Swettenham J, Rees L (1999) Children with Autism Show Local Precedence in a Divided Attention Task and Global Precedence in a Selective Attention Task. *Journal of Child Psychology and Psychiatry* 40:733-742.

8. Milne E et al. (2002) High motion coherence thresholds in children with autism. *Journal of Child Psychology and Psychiatry* 43(2):255-263.

9. Miles JH (2011) Autism spectrum disorders—A genetics review. *Genetics in Medicine* 13(4):278-294.

10. LeBlanc JJ et al. (2015) Visual evoked potentials detect cortical processing deficits in Rett syndrome. *Annals of Neurology* 78:775-786.

11. Burd L, Gascon GG (1988) Rett Syndrome: Review and Discussion of Current Diagnostic Criteria. *Journal of Child Neurology* 3:263-268.

12. West RJH, Furmstron R, Williams CAC, Elliott CJH (2015) Neurophysiology of Drosophila Models of Parkinson's Disease. *Parkinson's Disease* 2015:1-11.

13. Moloney A, Sattelle DB, Lomas DA, Crowther DC (2010) Alzheimer's disease: insights from Drosophila melanogaster models. *Trends in Biochemical Sciences* 35(4):228-235.

14. Reiter LT, Potocki L, Chien S, Gribskov M, Bier M (2001) A Systematic Analysis of Human Disease-Associated Gene Sequences In Drosophila melanogaster. *Genome Research* 11:1114-1125.

522 15. Fischbach K-F, Dittrich APM (1989) The optic lobe of Drosophila
523 melanogaster. I. A Golgi analysis of wild-type structure. *Cell and Tissue*
524 *Research* 258.

525 16. Behnia R, Desplan C (2015) Visual circuits in flies: beginning to see the
526 whole picture. *Current Opinion in Neurobiology* 34:125-132.

527 17. Afsari F et al. (2014) Abnormal visual gain control in a Parkinson's
528 disease model. *Human Molecular Genetics* 23(17):4465-4478.

529 18. Clark DA et al. (2014) Flies and humans share a motion estimation
530 strategy that exploits natural scene statistics. *Nature*
531 *Neuroscience* 17(2):296-303.

532 19. Kondapalli K, Hack A, Schushan M, Ben-Tal N, Rao R (2013) Functional
533 Evaluation of Autism Associated Mutations in NHE9. *Nature*
534 *Communications* 4(2510):1-12.

535 20. Skottun BC, Skoyles JR (2007) Some remarks on the use of visually
536 evoked potentials to measure magnocellular activity. *Clinical*
537 *Neurophysiology* 118:1903-1905.

538 21. Baron-Cohen S, Wheelwright, S, Skinner R, Martin J, Clubley E (2001)
539 The Autism-Spectrum Quotient (AQ): evidence from Asperger
540 Syndrome/high-functioning autism, males and females, scientists and
541 mathematicians. *Journal of Autism and Developmental Disorders* 31:5-17.

542 22. Lord C et al. (2000) The autism diagnostic observation schedule-generic:
543 a standard measure of social and communication deficits associated with
544 the spectrum of autism. *J Autism Dev Disord* 30:205-223.

545 23. Robertson AE, Simmons DR (2013) The Relationship between Sensory
546 Sensitivity and Autistic Traits in the General Population. *J Autism Dev*
547 *Disord* 43:775–784.

548 24. McKeefry DJ, Russell MHA, Murray IJ, Kulikowski JJ (1996) Amplitude
549 and phase variations of harmonic components in human achromatic and
550 chromatic visual evoked potentials. *Visual Neuroscience*13:639-653.

551 25. McLelland D, Baker PM, Ahmed B, Bair W (2010) Neuronal Responses
552 during and after the Presentation of Static Visual Stimuli in Macaque
553 Primary Visual Cortex. *Journal of Neuroscience* 30(38):12619-12631.

554 26. Pei F, Baldassi S, Norcia AM (2014) Electrophysiological measures of
555 low-level vision reveal spatial processing deficits and hemispheric
556 asymmetry in autism spectrum disorder. *Journal of Vision* 14(11):3-3.

557 27. Jemel B, Mimeault D, Saint-Amour D, Mottron L (2012) VEP contrast
558 sensitivity responses reveal reduced functional segregation of visual
559 processing channels in autism. *International Journal of*
560 *Psychophysiology* 10(6):85:298.

561 28. Schwede M, Garbett K, Mirnics K, Geschwind DH, Morrow EM (2013)
562 Genes for endosomal NHE6 and NHE9 are misregulated in autism
563 brains. *Molecular Psychiatry* 19:277-279.

29. Voineagu I et al. (2011) Transcriptomic analysis of autistic brain reveals convergent molecular pathology. *Nature* 474(7351):380-384.

30. Said CP, Egan RD, Minshew NJ, Behrmann M, Heeger DJ (2013) Normal binocular rivalry in autism: Implications for the excitation/inhibition imbalance hypothesis. *Vision Research* 77:59-66.

31. Dickinson A, Jones M, Milne E (2016) Measuring neural excitation and inhibition in autism: Different approaches, different findings and different interpretations. *Brain Research* 1648:277-289.

32. Simmons DR et al. (2009) Vision in autism spectrum disorders. *Vision Research* 49:2705-2739.

33. Greenaway R, Davis G, Plaisted-Grant K (2013) Marked selective impairment in autism on an index of magnocellular function. *Neuropsychologia* 51:592-600.

34. Sutherland A, Crewther DP (2010) Magnocellular visual evoked potential delay with high autism spectrum quotient yields a neural mechanism for altered perception. *Brain* 133:2089-2097.

35. Courchesne E, Redcay E, Kennedy DP (2004) The autistic brain: birth through adulthood. *Current Opinion in Neurology* 17:489-496.

36. Seltzer MM et al. (2003) The Symptoms of Autism Spectrum Disorders in Adolescence and Adulthood. *J Autism Dev Disord* 33(6):565-581.

37. Mcgovern CW, Sigman M (2005) Continuity and change from early childhood to adolescence in autism. *J Child Psychol Psychiatry* 46(4):401–408.

38. Pullikuth AK (2006) Molecular characterization of sodium/proton exchanger 3 (NHE3) from the yellow fever vector, Aedes aegypti. *Journal of Experimental Biology* 209:3529-3544.

39. Ben-Ari Y (2014) The GABA excitatory/inhibitory developmental sequence: A personal journey. *Neuroscience* 279:187-219.

40. Sharma P et al. (2005) Isogenic autisomes to be applied in optimal screening for novel mutants with viable phenotypes in Drosophila melanogaster. *Journal of Neurogenetics* 19:57-85.

41. Carpenter JM (1950) A new semisynthetic food medium for Drosophila. *Dros Inf Serv* 24:96-97.

599 ## Figure legends

600 **Figure 1. Human and *Drosophila* steady-state electrophysiology**
601 **methods.** Panel A illustrates an example of electrophysiological responses (in
602 the adult AQ dataset) as a function of time (red trace) in response to stimulus
603 flicker (black trace). Two peaks can be observed after each increase in
604 stimulus contrast giving rise to the first (1F) and second (2F) responses,
605 which are evident in the frequency domain after Fourier transform (lower
606 panel A). Adult participants (for both the autistic adult dataset and the
607 neurotypical AQ dataset) were presented with a grid of sinusoidal gratings
608 flickering at 7Hz whilst SSVEPs were recorded using a 64-channel EEG cap
609 (C). Children were tested with a binary noise stimulus flickering at 5.12Hz and
610 a 128-channel EEG cap (D). SSVEPs were measured from the occipital
611 electrode Oz (indicated by green dots in e, f, g) where the highest first
612 harmonic amplitude was centered, indicated by the heatmaps for the adult AQ
613 dataset (E), autistic adult dataset (F) and child dataset (G). Fruit fly
614 electrophysiological data were acquired as shown (B) using square wave
615 stimulus flicker; see Methods for more details.

616

617

618 **Figure 2. Older ASD-mimic flies and autistic humans have visual deficits**
619 **in the transient pathway.** Contrast response functions for adult *Nhe3* mutant
620 flies (*Nhe3*^{KG08307} homozygotes, red squares and *Nhe3*^{KG08307} */Df(2L)BSC187*,
621 purple diamonds) were similar at the first harmonic (a one-way ANOVA
622 showed no effect of group $F_{2,33} = 0.05$, $P = 0.95$, panel A) but responses were
623 reduced for P/P (simple contrast, P=0.025) and P/Df mutants compared to
624 controls at the second harmonic (simple contrast $P = 0.001$; ANOVA group
625 effect $F_{2,33} = 6.71$, $P < 0.01$; panel B). Ratios between frequencies ($\frac{1F-2F}{1F+2F}$)
626 were significantly higher for P/P ($P < 0.001$) and for P/Df ($P < 0.0001$) than for
627 the control genotype (C). First harmonic responses were also similar for the
628 high AQ and low AQ groups (panel D) and for autistic and neurotypical adults
629 (panel G). However, second harmonic responses were reduced for both
630 adults with high AQ (panel E) and autistic adults compared to controls (panels
631 H). The ratio between harmonics was also higher in both experimental groups
632 compared to controls (panels F and I, $P = 0.005$ and $P = 0.04$, respectively).
633 Curved lines are hyperbolic function fits to the data. Frequency ratios are
634 baselined in respect to the mean over groups of each comparison for display
635 purposes. Error bars in all panels represent ±SEM.
636

637

638 **Figure 3. Young ASD-mimic flies and autistic children have visual**
639 **deficits in the sustained pathway**. Young fruit flies showed reduced
640 responses at the first harmonic ($F_{2,33} = 3.73$, $P = 0.035$; panel A) with P/P and
641 P/Df flies showing a significant difference from control flies (respectively, P =

0.016 and P = 0.040). There was also a significant effect of genotype at the second harmonic ($F_{2,33}$ = 3.39, P = 0.046, panel B). P/Df flies showed a significant difference from control flies (P = 0.018), however, P/P showed a non-significant difference from controls (P = 0.064). The flies had normal frequency ratios (panel C). Autistic children also showed reduced first harmonic (t_{28} = 2.065, P = 0.048; panel D) but not second harmonic responses (t_{28} = 1.26, P = 0.22; panel E) and had frequency ratios similar to that of control children (t_{28} = 1.21, P = 0.24; panel F). Curved lines are hyperbolic function fits to the data. Frequency ratios are baselined in respect to the mean over groups of each comparison for display purposes. Error bars in all panels represent ±SEM.

Figure 4. Positive relationship between the number of autistic traits and first/second harmonic ratio. Scatterplot showing a significant positive relationship between AQ scores and frequency ratios in the 100 neurotypical adult dataset indicating a gradual increase of impairment with the number of reported autistic traits. The black line indicates the regression line of best fit. Shaded grey areas show histograms of AQ scores and frequency ratios. Blue-red color transition indicates number of AQ traits with participants split by median into low and high AQ groups as presented in *Fig. 2*.